Synthesis of Ordered Cubic Periodic Mesoporous Organosilicas with Ultra-Large Pores

Xufeng Zhou,[†,‡] Shizhang Qiao,*[,†] Na Hao,[‡] Xinglong Wang,[‡] Chengzhong Yu,[‡] Lianzhou Wang,[†] Dongyuan Zhao,*[,‡] and Gao Qing Lu[†]

ARC Centre for Functional Nanomaterials, School of Engineering and Australian Institute of Bioengineering and Nanotechnology, The University of Queensland, Brisbane 4072, Australia, and Department of Chemistry, Shanghai Key Laboratory of Molecular Catalysis and Innovative Materials and Laboratory of Advanced Materials, Fudan University, Shanghai 200433, People's Republic of China

Received December 17, 2006. Revised Manuscript Received February 2, 2007

Highly ordered ethylene bridged periodic mesoporous organosilica (PMO) materials with ultra-large pore sizes up to 14.7 nm were successfully synthesized by using triblock copolymer F127 as a template and 1,3,5-trimethylbenzene (TMB) as a swelling agent. SAXS and TEM measurements show that PMO products have a face-centered cubic (space group of $Fm\bar{3}m$) mesostructure. The influence of reaction temperature and acidity of the solution on the mesostructure of the PMO products were systematically studied. The pore size can be gradually expanded as the temperature decreases, and ordered PMOs can be obtained at a temperature even down to 5 °C with a relatively low acidity. As compared with mesoporous silica materials synthesized at identical conditions, our experimental results reveal that different hydrophobicity between precursors, bis(trimethoxysilyl)ethane and tetraethyl orthosilicate, may influence the swelling capacity of F127 micelles with TMB as well as the phase behavior of triblock copolymer F127, resulting in the different physicochemical properties of the final products.

Introduction

Since its first synthesis in 1999,[1−3] periodic mesoporous organosilica (PMO) materials have attracted increasing research attention in materials science. The high loading rate and uniform dispersion of the organic groups in frameworks, as well as various surface properties imparted from different functional groups, endow the PMO materials with unique advantages over mesoporous silica (MPS) and even their functionalized products. PMOs with different organic bridges,[4−10] mesostructures,[11−15] pore sizes,[16−19] and morphologies[20−26] have been successfully synthesized.

Taking the similar synthetic strategy of MPS materials, PMOs templated by cationic surfactants were first prepared.[1−7,20,27] The pore size was limited up to ∼5 nm because of the relatively short chain lengths of the templates. Inspired by the synthesis of large pore mesoporous silica using block copolymers as structure-directing agents, similar PMO materials with pore sizes ranging from 5 to 10 nm were prepared.[12−19,26,28,29] The pore size expanding methods that are efficient for MPS materials have been utilized for the attempt to prepare large pore PMOs. The pore size of 7 nm was achieved using cationic surfactants as templates with

* Corresponding authors. Prof. Dongyuan Zhao, Tel.: +86 21 55664194. Fax: +86 21 65641740. E-mail: dyzhao@fudan.edu.cn; Dr. Shizhang Qiao, Tel.: +61 7 33653885. Fax: +61 7 33656074. E-mail: s.qiao@uq.edu.au.

[†] The University of Queensland.

[‡] Fudan University.

(1) Asefa, T.; MacLachan, M. J.; Coombs, N.; Ozin, G. A. *Nature* **1999**, *402*, 867.
(2) Inagaki, S.; Guan, S.; Fukushima, Y.; Ohsuna, T.; Terasaki, O. *J. Am. Chem. Soc.* **1999**, *121*, 9611.
(3) Melde, B. J.; Holland, B. T.; Blanford, C. F.; Stein, A. *Chem. Mater.* **1999**, *11*, 3302.
(4) Yoshina-Ishii, C.; Asefa, T.; Coombs, N.; MacLachlan, M. J.; Ozin, G. A. *Chem. Commun.* **1999**, 2539.
(5) Asefa, T.; MacLachlan, M. J.; Grondey, H.; Coombs, N.; Ozin, G. A. *Angew. Chem., Int. Ed.* **2000**, *39*, 1808.
(6) Inagaki, S.; Guan, S.; Ohsuna, T.; Terasaki, O. *Nature* **2002**, *416*, 304.
(7) Kapoor, M. P.; Yang, Q. H.; Inagaki, S. *J. Am. Chem. Soc.* **2002**, *124*, 15176.
(8) Olkhovyk, O.; Jaroniec, M. *J. Am. Chem. Soc.* **2005**, *127*, 60.
(9) Burleigh, M. C.; Markowitz, M. A.; Jayasundera, S.; Spector, M. S.; Thomas, C. W.; Gaber, B. P. *J. Phys. Chem. B* **2003**, *107*, 12628.
(10) Hoffmann, F.; Cornelius, M.; Morell, J.; Froba, M. *Angew. Chem., Int. Ed.* **2006**, *45*, 3216.
(11) Sayari, A.; Hamoudi, S.; Yang, Y.; Moudrakovski, I. L.; Ripmeester, J. R. *Chem. Mater.* **2000**, *12*, 3857.
(12) Guo, W. P.; Kim, I.; Ha, C. S. *Chem. Commun.* **2003**, 2692.
(13) Zhang, Z. D.; Tian, B. Z.; Yan, X. X.; Shen, S. D.; Liu, X. Y.; Chen, D. H.; Zhu, G. S.; Zhao, D. Y.; Qiu, S. *Chem. Lett.* **2004**, *33*, 1132.
(14) Zhang, Z. D.; Yan, X. X.; Tian, B. Z.; Shen, S. D.; Chen, D. H.; Zhu, G. S.; Qiu, S. L.; Zhao, D. Y. *Chem. Lett.* **2005**, *34*, 182.
(15) Zhao, L.; Zhu, G. S.; Zhang, D. L.; Di, Y.; Chen, Y.; Terasaki, O.; Qiu, S. L. *J. Phys. Chem. B* **2005**, *109*, 764.
(16) Muth, O.; Schellbach, C.; Froba, M. *Chem. Commun.* **2001**, 2032.
(17) Zhu, H. G.; Jones, D. J.; Zajac, J.; Roziere, J.; Dutartre, R. *Chem. Commun.* **2001**, 2568.
(18) Guo, W. P.; Park, J. Y.; Oh, M. O.; Jeong, H. W.; Cho, W. J.; Kim, I.; Ha, C. S. *Chem. Mater.* **2003**, *15*, 2295.
(19) Bao, X. Y.; Zhao, X. S.; Li, X.; Chia, P. A.; Li, J. *J. Phys. Chem. B* **2004**, *108*, 4684.
(20) Lu, Y. F.; Fan, H. Y.; Doke, N.; Loy, D. A.; Assink, R. A.; LaVan, D. A.; Brinker, C. J. *J. Am. Chem. Soc.* **2000**, *122*, 5258.
(21) Guan, S.; Inagaki, S.; Ohsuna, T.; Terasaki, O. *J. Am. Chem. Soc.* **2000**, *122*, 5660.
(22) Kapoor, M. P.; Inagaki, S. *Chem. Mater.* **2002**, *14*, 3509.
(23) Kim, D. J.; Chung, J. S.; Ahn, W. S.; Kam, G. W.; Cheong, W. J. *Chem. Lett.* **2004**, *33*, 422.
(24) Rebbin, V.; Jakubowski, M.; Potz, S.; Froba, M. *Microporous Mesoporous Mater.* **2004**, *72*, 99.
(25) Kapoor, M. P.; Inagaki, S. *Chem. Lett.* **2004**, *33*, 88.
(26) Qiao, S. Z.; Yu, C. Z.; Xing, W.; Hu, Q. H.; Djojoputro, H.; Lu, G. Q. *Chem. Mater.* **2005**, *17*, 6172.
(27) Landskron, K.; Hatton, B. D.; Perovic, D. D.; Ozin, G. A. *Science* **2003**, *302*, 266.
(28) Bao, X. Y.; Zhao, X. S.; Qiao, S. Z.; Bhatia, S. K. *J. Phys. Chem. B* **2004**, *108*, 16441.
(29) Qiao, S. Z.; Yu, C. Z.; Hu, Q. H.; Jin, Y. G.; Zhou, X. F.; Zhao, X. S.; Lu, G. Q. *Microporous Mesoporous Mater.* **2006**, *91*, 59.

10.1021/cm062989f CCC: $37.00
Published on Web 03/13/2007

the 1,3,5-trimethylbenzene (TMB) as a pore expander.[30] The use of TMB in triblock copolymer F127 templated synthesis resulted in a pore size of 8 nm, but the ordered PMO mesostructure could not be obtained.[15,31] Hence, the pore sizes for ordered PMO materials reported so far are limited below 10 nm.[31]

Bis(trimethoxysilyl)ethane (BTME) and bis(triethoxysilyl)-ethane (BTEE) are two of the most commonly used precursors to synthesize PMOs because of their similarity in hydrolysis and condensation behaviors to a silica precursor, tetraethyl orthosilicate (TEOS), which is mostly used in the synthesis of MPS materials. Many PMO materials derived from the former two precursors were synthesized using similar experimental conditions to their pure silica counterparts.[2,3,11,20,26,29,32−36] However, the existence of the organic bridging group, $-CH_2CH_2-$, can influence the sol−gel process based on the induction and steric effects[37] to some extent. Furthermore, it has been found that some synthesis parameters for MPSs, especially the acidity that controls the hydrolysis and condensation rates (in the case of using block copolymers as templates), were required to be adjusted to meet the self-assembly of polysilsesquioxane species with templates.[19,26,28,29] Meanwhile, BTME and BTEE molecules have a higher hydrophobicity than TEOS. This difference may also affect the interaction between silicate precursors and templates that are amphiphilic in aqueous solution, but such an interaction is not well-understood.

The limited pore size of PMO materials may restrict their applications in some areas where ultra-large pores are in demand as substrates, such as the adsorption and immobilization of large biomolecules. Therefore, the expansion of the pore size for PMO materials continues to be a challenge in this area. In this paper, we adopted a low-temperature synthesis strategy that was developed previously in our group[38] to successfully prepare highly ordered face-centered cubic PMO materials with an ultra-large pore size (up to ~14.7 nm). To our knowledge, the products have the largest pore size ever reported for PMO materials. The influence of the synthesis temperature and the acidity of the solution on the mesostructure and morphology of PMO materials have been systematically investigated. It was found that the temperature to form ordered PMO products can be as low as 5 °C, which is much lower than their silica counterparts using the same template. Meanwhile, PMO materials prepared at 15 °C possess a hollow spherical morphology with ordered mesoporous shells, which may be good candidates for drug release and storage, separation, or chromatography.[39−42] As compared with MPS materials prepared at identical conditions, our results show the importance of the hydrophobicity of the inorganic precursor on the self-assembly of mesoporous materials.

Experimental Procedures

Synthesis. Bis(trimethoxysilyl)ethane (BTME, 96%) and triblock poly(ethylene oxide)-*b*-poly(propylene oxide)-*b*-poly(ethylene oxide) copolymer $EO_{106}PO_{70}EO_{106}$ (Pluronic F127, M_w = 13,400) were purchased from Aldrich. All chemicals were used as received without purification. In a typical synthesis, 0.5 g of F127 and 2.5 g of KCl were dissolved in 30 g of HCl (2 M). Then, 0.5 g of 1,3,5-trimethylbenzene (TMB) was poured into the solution and stirred for 6 h at a fixed temperature (T = 15, 12, 10, or 5 °C). Then, 2.0 g of BTME was added to the solution and stirred for 24 h at the same temperature, which was taken as the reaction temperature in the following text. The molar ratio of the reactants is F127/BTME/TMB/KCl/HCl/H_2O = 4.3×10^{-3}:1:0.56:4.5:8.1:225. The solution along with the precipitate was then removed to an autoclave and hydrothermally treated by putting in a 100 °C oven for another 24 h. The product was filtered and washed 2 times with ethanol and HCl (5.0 mL of 2 M HCl in 60 mL of ethanol) at 60 °C for 6 h to remove F127 template. The final PMO products were collected by filtration and dried in the air at room temperature.

In the synthesis using a mixture of BTME and TEOS as precursors, four groups of silica sources with different BTME/TEOS ratios were used: 1.733 g of TEOS + 0.333 g of BTME (0.148); 1.387 g of TEOS + 0.45 g of BTME (0.370); 1.04 g of TEOS + 0.675 g of BTME (0.740); and 0.693 g of TEOS + 0.9 g of BTME (1.478) (the values in the parentheses are molar ratios of BTME/TEOS), while keeping other conditions constant.

Characterization. Small-angle X-ray scattering (SAXS) measurements were performed on a Bruker NanoStar U small-angle X-ray scattering system using Cu Kα radiation at 40 kV and 35 mA. Transmission electron microscopy (TEM) images were obtained by a JEOL2010 electron microscope with an acceleration voltage of 200 kV. The powder samples for TEM measurements were suspended in ethanol, ground in a mortar, and then loaded onto the Cu grids with holey carbon films. Scanning electron microscopy (SEM) images were recorded on a JEOL 6400 microscope operating at 10 kV, and the samples were coated with platinum. Nitrogen sorption isotherms of samples were obtained by a Quantachrome's Quadrasorb SI analyzer at −196 °C. Before the measurements, the samples were degassed at 120 °C for 12 h in vacuum. The Brumauer−Emmett−Teller (BET) surface area was calculated using experimental points at a relative pressure of P/P_0 = 0.05−0.25. The total pore volume was calculated by the N_2 amount adsorbed at the highest P/P_0 for each sample (P/P_0 = 0.99). The pore size distribution was calculated by BdB methods, using a spherical pore model. The micropore area and volume were calculated by the *t*-plot method using experimental points at a relative pressure of P/P_0 = 0.10−0.20. The cross-polarization magic-angle spinning (CP-MAS) ^{29}Si NMR spectra with proton decoupling were acquired on a Bruker DSX 300 NMR spectrometer operating at a resonance frequency of 59.63 MHz and using Q_8M_8 ($[(CH_3)_3SiO]_8Si_8O_{12}$) as a reference.

(30) Liang, Y. C.; Anwander, R. *Microporous Mesoporous Mater.* **2004**, *72*, 153.
(31) Burleigh, M. C.; Markowitz, M. A.; Wong, E. M.; Lin, J. S.; Gaber, B. P. *Chem. Mater.* **2001**, *13*, 4411.
(32) Liang, Y. C.; Hanzlik, M.; Anwander, R. *Chem. Commun.* **2005**, 525.
(33) Hatton, B. D.; Landskron, K.; Whitnall, W.; Perovic, D. D.; Ozin, G. A. *Adv. Funct. Mater.* **2005**, *15*, 823.
(34) Liang, Y. C.; Hanzlik, M.; Anwander, R. *J. Mater. Chem.* **2005**, *15*, 3919.
(35) Xia, Y. D.; Yang, Z. X.; Mokaya, R. *Chem. Mater.* **2006**, *18*, 1141.
(36) Xia, Y. D.; Mokaya, R. *J. Phys. Chem. B* **2006**, *110*, 3889.
(37) Brinker, C. J.; Scherer, G. W. *Sol−Gel Science: The Physics and Chemistry of Sol−Gel Processing*; Academic Press: Boston, 1990.
(38) Fan, J.; Yu, C. Z.; Lei, J.; Zhang, Q.; Li, T. C.; Tu, B.; Zhou, W. Z.; Zhao, D. Y. *J. Am. Chem. Soc.* **2005**, *127*, 10794.
(39) Schacht, S.; Huo, Q.; VoigtMartin, I. G.; Stucky, G. D.; Schuth, F. *Science* **1996**, *273*, 768.
(40) Yin, Y.; Lu, Y.; Gates, B.; Xia, Y. *Chem. Mater.* **2001**, *13*, 1146.
(41) Li, Y. S.; Shi, J. L.; Hua, Z. L.; Chen, H. R.; Ruan, M. L.; Yan, D. S. *Nano Lett.* **2003**, *3*, 609.
(42) Djojoputro, H.; Zhou, X. F.; Qiao, S. Z.; Wang, L. Z.; Yu, C. Z.; Lu, G. Q. *J. Am. Chem. Soc.* **2006**, *128*, 6320.

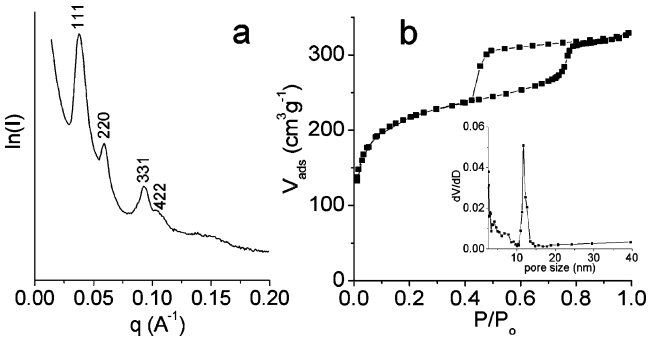

Figure 1. (a) SAXS pattern and (b) nitrogen sorption isotherms of the PMO material synthesized at 15 °C in 2 M HCl. Inset of panel b is its pore size distribution obtained by using the BdB sphere model.

Results

Highly ordered PMO materials with ultra-large pores can be prepared by using a low-temperature synthesis method. After the removal of templates by solvent extraction, at least four well-resolved diffraction peaks are observed in the SAXS pattern of the PMO sample prepared at a temperature of 15 °C and a HCl concentration of 2.0 M, which can be assigned to a face-centered cubic (fcc) mesostructure (space group $Fm\bar{3}m$) (Figure 1a). The cell parameter (a) calculated from the diffraction peaks is 28.9 nm. It is noted that the 200 diffraction peak for the $Fm\bar{3}m$ structure is not observed in the SAXS pattern of our PMO samples that may be due to small domain areas of the fcc mesostructure, which leads to a broadening of diffraction peaks and thus a overlay of the 200 diffraction peak with an adjacent and relatively strong 111 diffraction peak. Nitrogen sorption isotherms of the sample display a typical type IV adsorption isotherm of mesoporous materials with a type H2 hysteresis loop (Figure 1b), implying a cage-like pore structure connected by windows with a small size. The capillary condensation step in the adsorption branch is observed at relatively high pressure, indicating a large diameter of the cage. The BET surface area and total pore volume calculated are 736 m^2/g and 0.51 cm^3/g, respectively. The narrow pore size distribution calculated from the adsorption branch using the BdB sphere method suggests that the mesopores have uniform sizes. The pore size at the mean value of 11.7 nm is larger than any ordered PMO materials reported previously but still much smaller than the 22 nm MPS LP-FDU-12 synthesized at identical conditions.[38] It should be noted that the micropore area and volume calculated from the *t*-plot method for this PMO material are 322 m^2/g and 0.16 cm^3/g, respectively (Table 1), which are relatively larger than that for the MPS materials (LP-FDU-12). It may be attributed to a looser wall structure for PMOs caused by the ethylene group.

TEM images of the PMO sample recorded along the [100] and [110] zone axes (Figure 2a,b, respectively) further confirm an ordered fcc mesostructure. The cell parameter (a) measured from the TEM images is ~27 nm, which is coincident with the value from the SAXS data. The hexagonal close-packed (hcp) mesostructure, which often exists as an intergrowth phase with the fcc mesostructure, is not found either in SAXS or in TEM data. Therefore, the mesostructure of our PMO samples is clearly assigned to the fcc structure with a space group of $Fm\bar{3}m$.

Table 1. Structure Parameters of PMO Materials Synthesized at Different Temperatures and Acidities

synthetic temperature (°C)	*HCl (M)*	unit cell parameter *a* (nm)	pore size[a] (nm)	surface area[b] (m^2/g)	pore volume[c] (cm^3/g)	micropore volume[d] (cm^3/g)	micropore area[d] (m^2/g)
15	2.0	28.9	11.7	736	0.51	0.16	322
	1.5	28.9	11.7	711	0.52	0.16	337
	1.0	29.4	12.6	735	0.54	0.17	362
	0.2	28.3	10.2	769	0.57	0.18	376
12	2.0	31.2	13.3	792	0.56	0.18	355
	1.5	28.9	11.7	833	0.58	0.18	395
	1.0	28.9	12.1	831	0.60	0.19	398
	0.2	31.9	11.9	717	0.54	0.17	351
10	2.0	37.3	14.7	646	0.43	0.12	232
	1.5	31.2	13.2	680	0.48	0.16	327
	1.0	29.4	12.1	739	0.53	0.16	325
	0.2	30.6	12.7	525	0.48	0.10	212
5	2.0			803	0.48	0.08	148
	1.5	39.2[e]	18.5	686	0.44	0.11	226
	1.0	30.6[e]	13.9	688	0.50	0.16	330
	0.2	30.6	12.5	557	0.48	0.10	209

[a] Calculated by the BdB method, using a spherical pore model. [b] BET surface area calculated using experimental points at relative pressure of $P/P_0 = 0.05-0.25$. [c] Calculated by the N_2 amount adsorbed at the highest P/P_0 (~0.99). [d] Calculated by *t*-plot method using experimental points at relative pressure of $P/P_0 = 0.10-0.20$. [e] Cell parameter is calculated taking the first diffraction peak in SAXS data as the 111 scattering peak of the fcc structure.

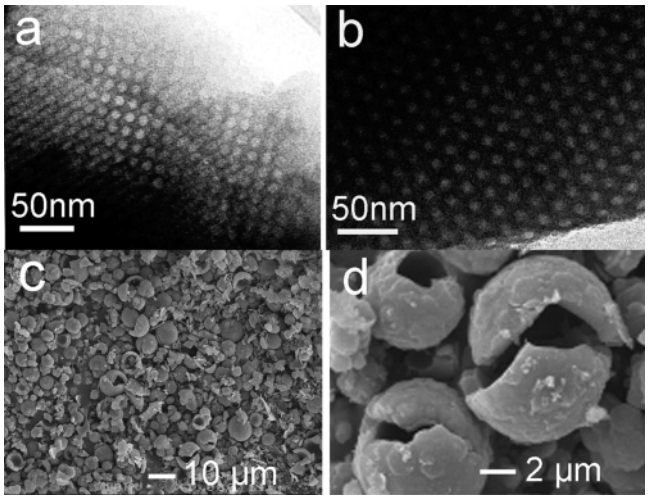

Figure 2. (a and b) TEM images viewed from [100] (a) and [110] (b) directions and (c and d) SEM images at different magnifications of the PMO material prepared by using triblock copolymer F127 as a template at 15 °C in 2 M HCl.

The SEM image of the PMO samples shows a large amount of spheres with diameters ranging from 2 to 10 μm (Figure 2c). Most of the spheres are not intact and exhibit a hollow interior. A higher magnification SEM image (Figure 2d) reveals that the thickness of the shells is ca. 1 μm and that the shells consist of small particles that can be distinguished from the outer surface of the hollow spheres.

The solid state ^{29}Si NMR spectrum (Figure 3) of the sample prepared at 15 °C in 2.0 M HCl shows two strong signals at −56.6 and −62.6 ppm, which can be assigned to the T^2 [C−Si(OH)(OSi)$_2$] and T^3 [C−Si(OSi)$_3$] Si species, respectively. Another relatively weak signal at ~48 ppm is also observed, corresponding to T^1 [C−Si(OH)$_2$(OSi)] Si. The strong intensity for the T^2 and T^3 signals indicates the formation of highly condensed organosilicate frameworks. No signal due to the Q^n [Si(OH)$_{4-n}$(OSi)$_n$] species is observed in the ^{29}Si NMR

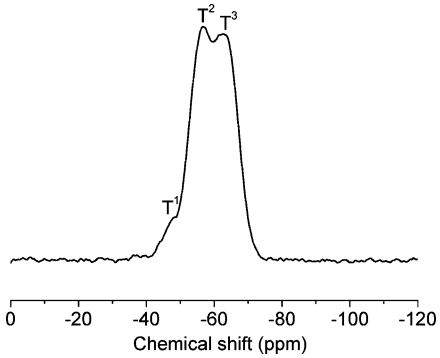

Figure 3. Solid state ^{29}Si NMR spectrum of the PMO sample prepared by using triblock copolymer F127 as a template at 15 °C in 2 M HCl.

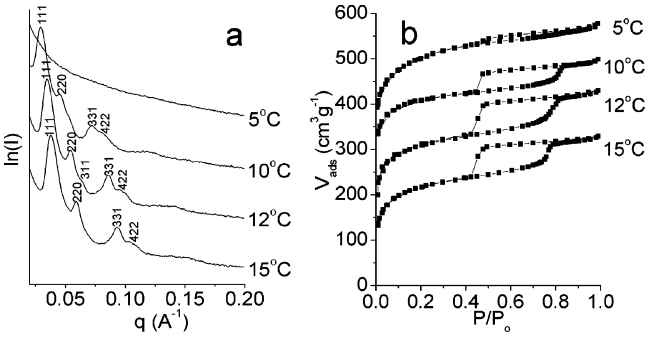

Figure 4. (a) SAXS patterns and (b) nitrogen sorption isotherms of PMO materials synthesized at different temperatures at the same acidity of 2 M HCl. The isotherms for the materials synthesized at 12, 10, and 5 °C in panel b are shifted by 100, 200, and 300 $cm^3\ g^{-1}$ STP, respectively, for clarity.

spectrum, indicating that the Si−C bonds are well-retained during the reaction process and the removal of templates.

The synthesis temperature can be further lowered to 5 °C. The SAXS pattern shows that the PMO material prepared at 12 °C in 2 M HCl also possesses a highly organized mesostructure (Figure 4a). The four peak resolved scattering pattern can also be assigned to the fcc mesostructure, and the calculated cell parameter (*a*) of 31.2 nm is larger than that for the sample synthesized at 15 °C. The fcc mesostrcture is maintained even at a temperature of 10 °C, and a four peak diffraction SAXS pattern can be observed. The cell parameter can be further enlarged to 37.2 nm. However, the scattering peaks become wide and less resolved, especially for the peaks at high *q* values, implying a decreased ordering of the mesostructure as the temperature decreases to 10 °C. Further decreasing the temperature to 5 °C, a disordered mesostructure without a scattering peak is obtained.

N_2 sorption measurements show that the samples prepared at both 12 and 10 °C have type IV adsorption isotherms and a type H2 hysteresis loop, indicating cage-like mesopores similar to that for the sample synthesized at 15 °C. Both of the samples also show a high BET surface area and pore volume, as well as a large amount of micropores (Table 1). More importantly, the relative pressures (P/P_0) at the capillary condensation step of the mesopores move to higher values, indicating an expansion of the mesopore size along with a decrease in the temperature. The pore diameter of the sample synthesized at 12 °C is 13.3 nm and is further enlarged to 14.7 nm for the sample prepared at 10 °C, which is the largest ever reported for PMO materials. When the

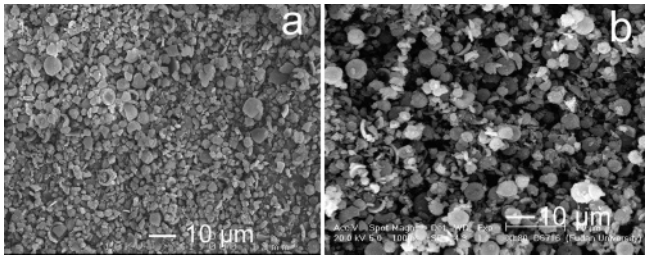

Figure 5. SEM images of samples synthesized at (a) 12 °C and (b) 10 °C in 2 M HCl solution.

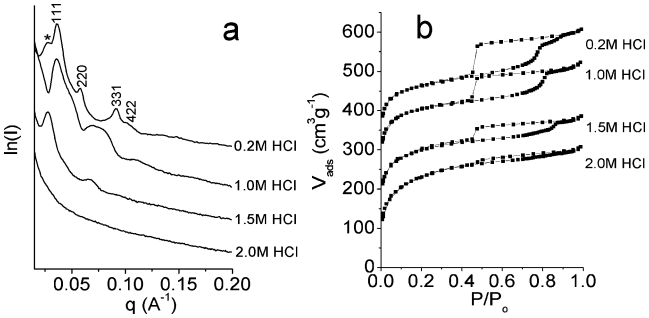

Figure 6. (a) SAXS patterns and (b) nitrogen sorption isotherms of PMO materials synthesized at 5 °C with different acidities. The isotherms for the materials synthesized in 1.5, 1.0, and 0.2 M HCl in panel b are shifted by 100, 200, and 300 $cm^3\ g^{-1}$ STP, respectively, for clarity.

temperature is further decreased to 5 °C, although the sample still has a high surface area and pore volume, no obvious capillary condensation at the mesopore range is observed, reflecting a collapse of the mesostructure, coincident with the SAXS data. Therefore, it is concluded that the lowest temperature to obtain ordered PMOs in our case is around 10 °C.

Accompanied by the pore expansion, samples synthesized at lower temperatures of 12 and 10 °C show a slightly different morphology from that of the sample prepared at 15 °C. SEM images of the former two samples (Figure 5) show that the amount of hollow spheres decreases while the amount of small solid particles with no regular morphology increases.

The mesostructural regularity of the PMO materials can be affected by the acidity of the solution.[19,26,28,29] In our system, a different HCl concentration (1.5, 1.0, and 0.2 M) was used at each temperature to prepare PMO materials, and the structure parameters of all samples are summarized in Table 1. SAXS and N_2 sorption measurements (not shown here) show that the ordered fcc mesostructures of samples synthesized at 15, 12, and 10 °C are maintained at all HCl concentrations. All samples have a high surface area and large pore volume. The HCl concentration has little influence on the cell parameters and pore sizes for samples prepared at 15 and 12 °C, both varying in the range of ±10%. A relatively obvious change of the cell parameters and pore sizes occurs at 10 °C.

It should be noted that HCl has a great effect on the formation of the mesostructure at a temperature of 5 °C. When the concentration decreases to 1.5 M HCl, two broad diffraction peaks appear in the SAXS pattern (Figure 6a). Although the peaks cannot be indexed, this implies the appearance of organized mesostructures to some extent. Further decreasing the HCl concentration to 1.0 M, more

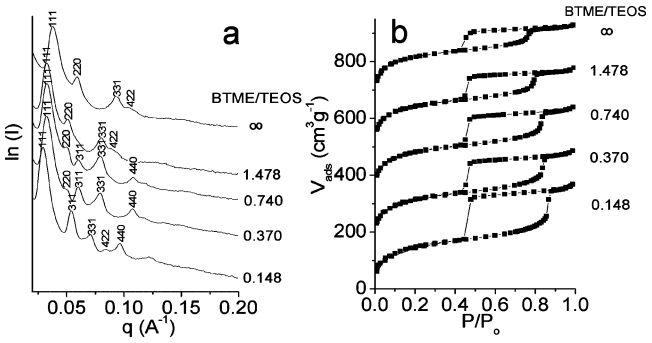

Figure 7. (a) SAXS patterns and (b) nitrogen sorption isotherms of PMO materials synthesized at 15 °C in 2.0 M HCl with different ratios of BTME/TEOS. The *y*-axis values of the isotherms for the materials synthesized at the BTME/TEOS ratio of 0.370, 0.740, 1.478, and ∞ in panel b are shifted by 150, 300, 450, and 600 cm^3 g^{-1}, respectively, for clarity.

diffraction peaks are observed, although they are quite broad and difficult to index. Finally, at least five resolved scattering peaks can be observed with 0.2 M HCl. Except the first peak (marked by an asterisk in Figure 6a), the rest of the four peaks can be assigned to the fcc mesostructure. The first diffraction peak cannot be indexed at the moment, implying the existence of a mixed mesophase. The nitrogen sorption isotherms of the samples also reveal an improvement of the mesostructural regularity when the acidity decreases (Figure 6b). The height of the hysteresis loop rises as the HCl concentration decreases, while the capillary condensation step in the adsorption branch shifts to low relative pressure, indicating a shrinkage of the pore sizes as listed in Table 1. Although the pore size of the sample obtained in 1.5 M HCl is calculated to be 18.5 nm, the mesostructure is poor according to the SAXS and N_2 sorption data and should not be considered as a high quality PMO material. The low acidity (0.2 M HCl) gives rise to a great improvement in the mesostructure; however, the expansion of the pore size by the swelling of TMB is limited.

Despite that identical experimental conditions were employed, the obtained PMO materials have apparent differences from their pure silica counterpart, LP-FDU-12, especially in the pore size, microporous surface area, and volume. To further understand the effects of the precursors, a series of samples was synthesized using the mixture of BTME and TEOS as a precursor at different molar ratios, at 15 °C in 2.0 M HCl. It should be mentioned that the molar amount of Si used in the synthesis of PMO materials is ca. 50% larger than that in the synthesis of LP-FDU-12 (because each BTME molecule contains two Si atoms). We have tried using the same amount of Si, but only randomly packed hollow spheres with diameters of around 15 nm were obtained without an ordered mesostructure. Therefore, 0.74 mol of BTME was taken to be as effective as 1 mol of TEOS to form a highly ordered mesostructure.

SAXS patterns (Figure 7a) show that all samples synthesized at different molar ratios of BTME/TEOS have a highly ordered fcc mesostructure. The scattering peaks gradually move to higher *q* values as the ratio increases (∞ means pure BTME), indicating a decrease of the unit cell parameter (Table 2). The *a* value of PMO derived from pure BTME is ~23% smaller than that of the sample prepared at a ratio of 0.148. Meanwhile, the pore sizes of the materials derived from the adsorption branches of the isotherms also continuously decrease from 18.9 to 11.7 nm as the BTME content increases (Figure 7b and Table 2). The BET surface area increases as an increment of the ratio while the total pore volume does not change much. The *t*-plot analysis reveals that the micropore volume and surface area gradually increase as the BTME/TEOS ratio increases, suggesting that the ethylene group in BTME is responsible for the origination of micropores under our experimental conditions. The increase of the BET surface area is ascribed to the increase of the micropore area.

It is interesting to note that the relative intensities of some diffraction peaks also vary along with the change of the ratio, especially for the 220 and 311 diffraction peaks. The 220 diffraction peak is not observed at the lowest BTME/TEOS ratio of 0.148, while the 311 diffraction peak cannot be discerned in the case of pure BTME. In between, the intensity of the 220 diffraction peak increases, and that of the 311 diffraction peak decreases as the BTME/TEOS ratio increases. Such variation has been reported previously in the synthesis of mesostructured silica, which is attributed to the variation of the matter distribution in the unit cell brought about by the change of structure parameters, such as pore size, entrance size, and ratio of pore size or entrance size to unit cell parameter.[43,44] For our samples, several obvious evolution trends of structural parameters with the increase of the BTME/TEOS ratio are observed, including a decrease of pore size, mesoporosity, and ratio of pore size to unit cell parameter and an increase of micropore area and microporosity (Table 2). All these regular variations certainly relate to a continuous evolution of matter distribution in one unit cell and thus lead to a continuous variation of intensities of diffraction peaks in SAXS as observed in Figure 7a.

The morphology of products with the variation of the BTME/TEOS ratio was investigated by SEM (Figure 8). At a ratio of 0.148, the PMO material is composed of solid particles with a size around 5 μm (Figure 8a). Many of the particles display a regular hexagonal shape, reflecting an ordered mesostructure (Figure 8a inset). A hollow sphere morphology is hardly observed in this sample, even in the sample synthesized at a ratio of 0.370 (Figure 8b). When the ratio is increased to 0.740, both solid particles and hollow spheres can be observed (Figure 8c), and the hollow spherical morphology becomes dominant while the ratio is further increased to 1.478 (Figure 8d).

The systematic evolution of the pore size, cell parameter, and morphology of the materials using mixed precursors at an increasing molar ratio of BTME/TEOS strongly suggests the different properties between BTME and TEOS and may shed some light on their different interactions with F127 and TMB during the formation of the mesostructure. Meanwhile, it provides a way to produce mesostructured organosilica materials with a tunable pore size.

(43) Kleitz, F.; Liu, D. N.; Anilkumar, G. M.; Park, I. S.; Solovyov, L. A.; Shmakov, A. N.; Ryoo, R. *J. Phys. Chem. B* **2003**, *107*, 14296.
(44) Yu, T.; Zhang, H.; Yan, X. W.; Chen, Z. X.; Zou, X. D.; Oleynikov, P.; Zhao, D. Y. *J. Phys. Chem. B* **2006**, *110*, 21467.

Table 2. Structure Parameters of PMO Materials Synthesized at Different Molar Ratios of BTME/TEOS

BTME/TEOS	*cell parameter a* (nm)	pore size (nm)	surface area (m^2/g)	pore volume (cm^3/g)	mesoporosity[a] (%)	micropore volume (cm^3/g)[b]	micropore area (m^2/g)[b]	*pore size vs* unit cell[c]
0.148	37.3	18.9	534	0.57	27.2	0.01	30	0.51
0.370	34.0	16.8	573	0.52	25.3	0.04	91	0.49
0.740	33.3	15.9	636	0.53	22.8	0.12	260	0.48
1.478	33.3	13.7	661	0.51	14.6	0.12	237	0.41
	28.9	11.7	736	0.54	13.9	0.16	322	0.40

[a] Calculated by the equation $(16/3\pi r^3)/a^3$, where r is the mesopore radius and a is the cell parameter. [b] Calculated by *t*-plot method. [c] Pore size divided by unit cell parameter.

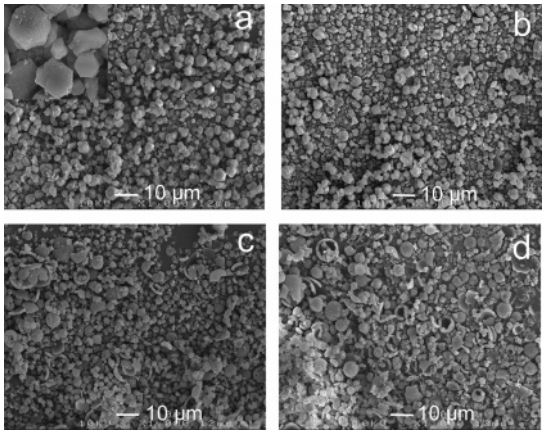

Figure 8. SEM images of PMO materials synthesized at the BTME/TEOS molar ratio of (a) 0.148, (b) 0.370, (c) 0.740, and (d) 1.478.

Discussion

Our results show that the pore size of the ethylene bridged PMO materials with a highly ordered fcc mesostructure can be enlarged to 14.7 nm, the largest ever reported, using a low-temperature synthesis strategy. A pore expansion trend with a decrease of the temperature is also observed. A low temperature of 10−15 °C used in our experiments is an effective range for the penetration of TMB molecules into hydrophobic cores of F127 micelles. It has been reported that the association number of micelles reduces when it approaches the critical micelle temperature (CMT) and that the copolymer molecules are less tightly aggregated in one micelle,[45,46] which benefits the penetration of TMB into hydrophobic cores. The existence of TMB simultaneously lowers the CMT of block copolymers, resulting in expanded micelles at relatively low temperatures. Therefore, pore enlarged PMO materials can be successfully obtained from 10−15 °C, until no micelle is formed at lower temperatures, such as 5 °C in the solution of 2 M HCl.

Similar temperature-dependent pore expansion has been observed previously for mesoporous silica LP-FDU-12 with ultra-large pores.[38] However, the differences in the two cases are obvious, including the pore size and the lowest temperature to obtain organized mesostructures. Since the only difference between the two cases is the precursor, it is natural to ascribe the distinct experimental results to the difference between BTME and TEOS. Meanwhile, the continuous evolution of the cell parameters and pore sizes of materials prepared with different BTME/TEOS ratios also gives some clues as to the difference between two precursors.

Because of the different pore diameters in the two synthetic systems, there must exist a recombination of all species in the solution after the addition of silica precursors, BTME or TEOS, rather than a direct deposition of silica species on preformed swelled F127 micelles. Therefore, BTME or TEOS as well as their derivatives after the hydrolysis and condensation should be taken into account during the formation of swelled micelles. The existence of ethylene bridges makes BTME molecules more hydrophobic than TEOS, which can affect the interaction between F127 and TMB molecules. Although detailed information on a molecular scale cannot be obtained at this stage, it is reasonable to deduce that the existence of BTME may favor a tight aggregation of F127 molecules in a micelle as compared to that for TEOS. This may be easily understood with weak interactions between BTME and triblock copolymer F127 molecules due to the organic group in the silicate species; therefore, the organization of the loose silicate species derived from BTME and tight micelles aggregated from the F127 molecules is favorable. Therefore, the penetration of TMB is limited, and thus, the pore size of the PMO materials is smaller than that for TEOS. Consequently, our PMO materials can be attained at 10 °C in a solution of 2.0 M HCl and even down to 5 °C if the acidity is further reduced to 0.2 M HCl, while only disordered products were obtained below 14 °C, and no precipitate was observed below 10 °C in the case of LP-FDU-12. On the other hand, the ethylene group can induce steric effects, which may suppress the entering of the TMB molecules into the cores with their hydrophobicity. This simultaneously leads to the formation of a large amount of micropores on the PMO walls.

As only part of the TMB molecules is involved in the swelling F127 molecules, the rest remaining in the bulk solution tend to form oil/water emulsions assisted by amphiphilic F127 molecules, which serve as templates for the formation of hollow sphere mesoporous hybrids.[39] The more TMB swells the micelles, the less is left in the solution at a constant TMB concentration. Consequently, samples with larger pores should possess less hollow spheres, and this is observed for samples prepared at different temperatures and those with different BTME/TEOS ratios.

The acidity is another important factor to affect the self-assembly process. The PEO segments of F127 tend to be protonated in acid solution. When the HCl concentration decreases from 2.0 to 0.2 M, the PEO moieties become more hydrophobic because of less protonation. Although the concentration of Cl^- decreases at the same time, which can increase the hydrophilicity of F127, the decrease of H^+ (from 2 to 0.2 M) is more than 4 times larger than that of Cl^- (from 3.1 to 1.3 M, considering Cl^- in both HCl and KCl);

(45) Mortensen, K.; Pedersen, J. S. *Macromolecules* **1993**, *26*, 805.
(46) Booth, C.; Attwood, D. *Macromol. Rapid Commun.* **2000**, *21*, 501.

thus, the CMT for F127 decreases. Therefore, ordered PMO materials could be formed at 5 °C with 0.2 M HCl. On the other hand, the less protonated PEO segments at relatively lower acidity can reduce their repulsion between each other, resulting in a tight aggregation of F127 molecules in one micelle that subsequently blocks the penetration of TMB molecules. Accordingly, the pore sizes of the PMO materials become smaller along with the reduction of the acidity, especially at 10 and 5 °C. In addition, the low acidity also slows down the hydrolysis rate of BTME, which has been proven to be helpful for the fabrication of a highly ordered mesostructure of PMO materials using triblock copolymers as templates.[28,29]

Conclusion

At low temperatures from 5 to 15 °C, highly ordered PMO materials with an fcc mesostructure and ultra-large pores are obtained by using BTME as a precursor, F127 as a template, and TMB as a swelling agent. A continuous pore expansion along with a decrease of temperature is observed. The pore size of 14.7 nm prepared at 10 °C is the largest among all ordered PMO materials reported so far. By reducing the acidity of the reaction solution, PMO materials can be attained even when the temperature goes down to 5 °C. Meanwhile, the PMO materials synthesized at 15 °C possess a hollow spherical morphology with an ordered mesoporous shell. The pore size of our PMO materials is much smaller than their silica counterpart LP-FDU-12. However, ordered PMO materials can be obtained at a lower temperature than MPS materials, and they have a much higher micropore area and volume. Higher hydrophobicity of BTME than TEOS is believed to be the key factor that influences the swelling of F127 micelles and their further self-assembly behaviors into ordered mesostructures, resulting in different properties of the final products. The study of the distinction between BTME and TEOS in this work is also insightful for the understanding of the sol−gel and self-assembly science of organosilicate systems.

Acknowledgment. This work was financially supported by the Australian Research Council (ARC) through the Discovery Project Program (DP0452461, APD fellowship for S.Q.); UQ Early Career Researcher Grant (20041423); NSF of China (20373013, 20421303, and 20521140450); State Key Basic Research Program of PRC (2006CB202502 and 2006CB0N0302); and the Shanghai Science and Technology Committee (05DZ-22313, 06DJ14006, and 04JC14087). Financial support from the ARC for the ARC Centre for Functional Nanomaterials is also acknowledged.

CM062989F